AFRL-AFOSR-VA-TR-2016-0163

Quantum Metaphotonics

Galina Khitrova
ARIZONA UNIV BOARD OF REGENTS TUCSON

03/24/2016
Final Report

Air Force Research Laboratory
AF Office Of Scientific Research (AFOSR)/ RTA1
Arlington, Virginia 22203
Air Force Materiel Command

REPORT DOCUMENTATION PAGE

Form Approved
OMB No. 0704-0188

PLEASE DO NOT RETURN YOUR FORM TO THE ABOVE ORGANIZATION.

1. REPORT DATE *(DD-MM-YYYY)*	2. REPORT TYPE	3. DATES COVERED *(From - To)*
	Final Report	Oct. 2012 - Oct. 2015

4. TITLE AND SUBTITLE
Quantum Metaphotonics

5a. CONTRACT NUMBER
FA9550-13-1-0003

5b. GRANT NUMBER

5c. PROGRAM ELEMENT NUMBER

6. AUTHOR(S)
Khitrova, Galina

5d. PROJECT NUMBER

5e. TASK NUMBER

5f. WORK UNIT NUMBER

7. PERFORMING ORGANIZATION NAME(S) AND ADDRESS(ES)
University of Arizona
Meinel Bldg 94
1630 E. University Blvd.
Tucson, AZ 85721

8. PERFORMING ORGANIZATION REPORT NUMBER

9. SPONSORING/MONITORING AGENCY NAME(S) AND ADDRESS(ES)
Program Manager: Dr. Gernot Pomrenke
AF Office of Scientific Research
875 North Randolph Street, Room 3112
Arlington, VA 22203

10. SPONSOR/MONITOR'S ACRONYM(S)

11. SPONSOR/MONITOR'S REPORT NUMBER(S)

12. DISTRIBUTION/AVAILABILITY STATEMENT
Approved for public release; distribution is unlimited.

13. SUPPLEMENTARY NOTES

14. ABSTRACT

Under the completed AFOSR grant we investigated the light-matter coupling between plasmonic nano-antennas and near-surface quantum confined structures. This included optimizing the MBE growth conditions of a near-surface quantum wells with emission around 1500nm and fabrication of arrays of various resonant antenna structures. Pump-probe spectroscopy was used to investigate the coupling effects, and a toy model was used to extract the coupling parameters. Utilizing antennas with a higher dipole moment, such as square patch antennas, is counteracted by the decrease in packing efficiency and the increase in the local density of optical states of these antennas and thus reducing the effective coupling.

To move towards observing coupling between plasmonic nano-antennas and high quality quantum dots we investigated self-assembled MBE grown indium plasmonic nanostructures, or indium islands. Low densities of indium islands have been shown to increase the photoluminescence of an ensemble of InAs quantum dots. Indium islands have also been shown to be superconduting showing promise for possible superconducting plasmonics such as superconductor/semiconductor hybrid sources.

15. SUBJECT TERMS

16. SECURITY CLASSIFICATION OF:			17. LIMITATION OF ABSTRACT	18. NUMBER OF PAGES	19a. NAME OF RESPONSIBLE PERSON
a. REPORT	b. ABSTRACT	c. THIS PAGE			Galina Khitrova
U	U	U	UU		19b. TELEPHONE NUMBER *(Include area code)* (520) 834-3595

Reset

INSTRUCTIONS FOR COMPLETING SF 298

1. REPORT DATE. Full publication date, including day, month, if available. Must cite at least the year and be Year 2000 compliant, e.g. 30-06-1998; xx-06-1998; xx-xx-1998.

2. REPORT TYPE. State the type of report, such as final, technical, interim, memorandum, master's thesis, progress, quarterly, research, special, group study, etc.

3. DATES COVERED. Indicate the time during which the work was performed and the report was written, e.g., Jun 1997 - Jun 1998; 1-10 Jun 1996; May - Nov 1998; Nov 1998.

4. TITLE. Enter title and subtitle with volume number and part number, if applicable. On classified documents, enter the title classification in parentheses.

5a. CONTRACT NUMBER. Enter all contract numbers as they appear in the report, e.g. F33615-86-C-5169.

5b. GRANT NUMBER. Enter all grant numbers as they appear in the report, e.g. AFOSR-82-1234.

5c. PROGRAM ELEMENT NUMBER. Enter all program element numbers as they appear in the report, e.g. 61101A.

5d. PROJECT NUMBER. Enter all project numbers as they appear in the report, e.g. 1F665702D1257; ILIR.

5e. TASK NUMBER. Enter all task numbers as they appear in the report, e.g. 05; RF0330201; T4112.

5f. WORK UNIT NUMBER. Enter all work unit numbers as they appear in the report, e.g. 001; AFAPL30480105.

6. AUTHOR(S). Enter name(s) of person(s) responsible for writing the report, performing the research, or credited with the content of the report. The form of entry is the last name, first name, middle initial, and additional qualifiers separated by commas, e.g. Smith, Richard, J, Jr.

7. PERFORMING ORGANIZATION NAME(S) AND ADDRESS(ES). Self-explanatory.

8. PERFORMING ORGANIZATION REPORT NUMBER. Enter all unique alphanumeric report numbers assigned by the performing organization, e.g. BRL-1234; AFWL-TR-85-4017-Vol-21-PT-2.

9. SPONSORING/MONITORING AGENCY NAME(S) AND ADDRESS(ES). Enter the name and address of the organization(s) financially responsible for and monitoring the work.

10. SPONSOR/MONITOR'S ACRONYM(S). Enter, if available, e.g. BRL, ARDEC, NADC.

11. SPONSOR/MONITOR'S REPORT NUMBER(S). Enter report number as assigned by the sponsoring/ monitoring agency, if available, e.g. BRL-TR-829; -215.

12. DISTRIBUTION/AVAILABILITY STATEMENT. Use agency-mandated availability statements to indicate the public availability or distribution limitations of the report. If additional limitations/ restrictions or special markings are indicated, follow agency authorization procedures, e.g. RD/FRD, PROPIN, ITAR, etc. Include copyright information.

13. SUPPLEMENTARY NOTES. Enter information not included elsewhere such as: prepared in cooperation with; translation of; report supersedes; old edition number, etc.

14. ABSTRACT. A brief (approximately 200 words) factual summary of the most significant information.

15. SUBJECT TERMS. Key words or phrases identifying major concepts in the report.

16. SECURITY CLASSIFICATION. Enter security classification in accordance with security classification regulations, e.g. U, C, S, etc. If this form contains classified information, stamp classification level on the top and bottom of this page.

17. LIMITATION OF ABSTRACT. This block must be completed to assign a distribution limitation to the abstract. Enter UU (Unclassified Unlimited) or SAR (Same as Report). An entry in this block is necessary if the abstract is to be limited.

Quantum Metaphotonics

FINAL REPORT
March 2016
For October 15, 2012 through October 14, 2015

Galina Khitrova, PhD
College of Optical Sciences
University of Arizona
Tucson, Arizona 85721
khitrova@att.net

US Air Force Office of Scientific Research
Grant No. FA9550-13-1-0003
APPROVED FOR PUBLIC RELEASE
DISTRIBUTION UNLIMITED

Executive Summary

Under the completed AFOSR grant we investigated the light-matter coupling between plasmonic nano-antennas and near-surface quantum-confined structures. This included optimizing the molecular beam epitaxy growth conditions of a near-surface quantum well with emission around 1500 nm and fabrication of arrays of various resonant antenna structures. Pump-probe spectroscopy was used to investigate the coupling effects, and a toy model [1; 2] was used to extract the coupling parameters. Utilizing antennas with a higher dipole moment, such as square patch antennas, is counteracted by the decrease in packing efficiency and the increase in the local density of optical states of these antennas and thus reducing the effective coupling.

To move towards observing coupling between plasmonic nano-antennas and high quality quantum dots we investigated self-assembled MBE grown indium plasmonic nanostructures, or indium islands. While quantum dots degrade more significantly as they are in closer proximity to the surface compared to quantum wells, the improved interface between the semiconductor and the plasmonic structure, due to the single process epitaxial growth, increases the interaction. Low densities of indium islands have been shown to increase the photoluminescence of InAs quantum dots capped by 7 nm of GaAs. At this separation the quantum dots are broadened significantly such that individual emitters can't be distinguished from the ensemble of quantum dots. However, utilizing the superconductivity of indium can increase this interaction distance through the proximity effect allowing for the interaction of Cooper pairs with hole pairs in quantum-confined structures. Indium islands have been shown to be superconducting and are a promising candidate for superconductor/semiconductor hybrid source.

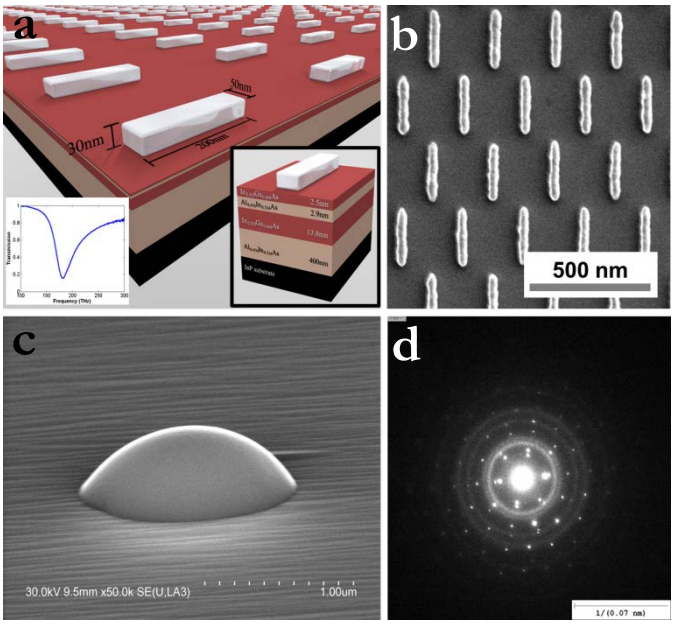

Figure 1: (a) Diagram of an array of silver wire antennas fabricated on top of a near-surface quantum well. (Inset left) Typical transmission spectrum of a wire nano-antenna. (Inset right) Close-up of the quantum well structure. (b) An actual array of EBL fabricated staggered nano-antennas. (c) A scanning electron microscope (SEM) image of a large self-assembled indium island. (d) The high quality growth of indium islands results in structures that are crystalline, demonstrated by the clear diffraction pattern.

Introduction

Motivated by our focus on enhancing light-matter coupling and our ability and experience of fabricating metallic structures on our epitaxially grown quantum-confined heterostructures, via molecular beam epitaxy (MBE) in the form of quantum wells (QWs) and quantum dots (QDs), we sought to continue our investigation of hybrid metal-semiconductor nanosystems where individual quanta play a decisive role.

Subwavelength metallic nano-antennas are able to confine optical excitations as surface plasmons to a volume about 1000 times smaller than $(\lambda/n)^3$ [3, 4]. This highly localized field can act on quantum emitters within the evanescent tail of the field, leading to modified spontaneous emission properties. This nanolocalized source was proposed in [5] and called a spaser (surface plasmon amplification by stimulated emission of radiation). Unlike the narrow (high Q) resonances of photonic crystals, metallic resonators have Q's of around 10. This allows the resonance to spectrally overlap with more than one quantum dot at a time. Since the Purcell enhancement goes as Q/V, we see the same enhancement as a photonic crystal cavity, which has a Q around 10,000. The metallic resonator acts as a short-lived storage device, somewhat like an optical cavity. Interestingly, the optical resonance frequency can be changed by the shape and size of the metallic resonator: the smaller it is, the shorter its resonance wavelength. When an array is fabricated with the distance between resonators about the same as their size, they couple with each other resulting in a collective mode. With the fabrication on top of quantum wells or quantum dots beneath but close to the surface, one could hope for coupling between the resonators and quantum-confined emitters.

This led us to examine the potential of such metallic resonator arrays. Our group's quest for and success in achieving single quantum dot vacuum Rabi splitting in 2004 (quantum strong coupling, currently 1,354 citations) [6, 7] was preceded by the study of normal mode coupling (NMC) between the excitonic resonance of QWs and a single mode of a planar microcavity [8]. We understood much of the physics by considering the NMC as simply two coupled oscillators. Similarly, it seemed logical to begin the study of metallic resonators by using an array of them on top of samples with QWs or QDs grown close to the surface using our MBE machine. The field of these cavities falls off exponentially on a length scale of ~10 nm, see figure 2 [9]. In order to couple to this field a quantum dot or quantum well must be positioned within this short distance from the surface of the semiconductor. The poor quality of a semiconductor surface can cause increased non-radiative recombination, leading to decreased photoluminescence and shorter carrier lifetimes, both undesirable qualities.

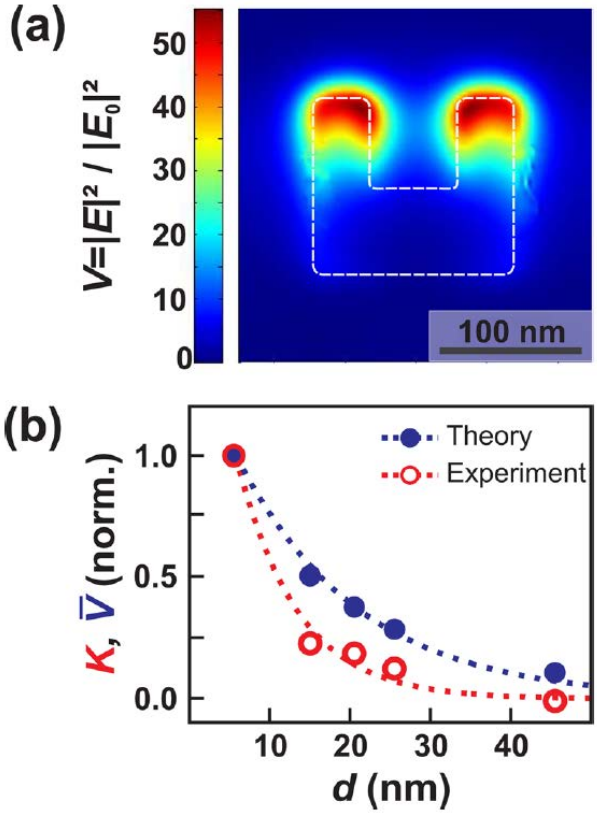

Figure 2: Example of numerically calculated near-field enhancement ($V = |\mathbf{E}|^2/|\mathbf{E_0}|^2$); the cut plane shown corresponds to the midplane of the QW in the sample with d = 5.5 nm. The dashed white outline marks the dimension of the SRR. (b) Dependence of normalized experimental and numerical coupling measures K and V versus distance d. The dotted lines show exponential fits to the data. [9]

When a quantum-confined gain material is pumped strongly, the near-field coupled system can be thought of as coupling between a metallic resonator oscillator and a second oscillator providing gain (roughly centered on the photoluminescence peak). We wanted to understand the dependence of the dipole moment on the size and shape of the metallic structure, as well as how the collective dipole moment of an array of metallic nano-antennas changes due to the coupling between the individual antennas. The interesting thing is that one can think of this array of metallic antennas as an array of meta-atoms whose spacing and interactions can be precisely controlled through fabrication. The nano-antenna patterns are written by electron-beam lithography into a PMMA mask, after which the sample is coated with silver. A chemical lift-off procedure is used to remove excess silver, leaving behind arrays of silver nano-antennas. To determine the quality of the samples, they are characterized by scanning electron microscopy (SEM) and Fourier transform infrared (FTIR) spectroscopy.

Quantum Well-Antenna Coupled System

From our previous grant, and in collaboration with the group of Prof. Martin Wegener, we investigated the coupling of nano-antennas in the form of split-ring resonators (SRRs) coupled to a near surface quantum well [10]. The SRRs sizes were varied, shifting the resonances, but the overall shape remained the same. Wegener's group went on to determine, using extinction cross-section

measurements of single metallic structures, that the ratio of radiative to non-radiative cross section contributions can be increased by changing the shape from a SRR to a straight nanorod, see figure 3 [11]. While the metal used in that work was gold, the basic principle is the same. Based on this observation, and with the goal of increasing the radiative contribution and reducing ohmic losses, we began exploring different shapes and arrangements of nano-antennas. Our work, discussed below, resulted in a publication in the Journal of Optics [1].

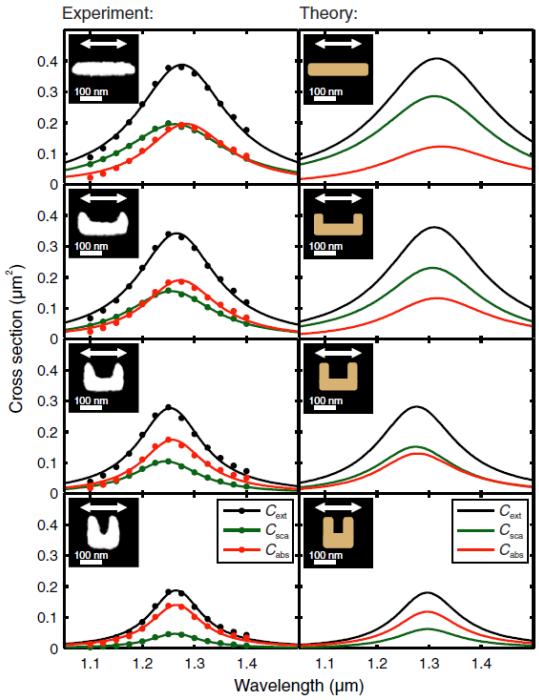

Figure 3: Transition from a straight dipole antenna (top) to a split-ring resonator (bottom). In the left column, the dots show the measured scattering C_{sca} (green), absorption C_{abs} (red), and extinction cross-section spectra C_{ext} (black). The solid curves result from Lorentzian fits. The insets show electron micrographs of the 35 nm thin gold nano-antennas. For all cases, the incident linear polarization is horizontal (see double arrow). The results of corresponding numerical calculations are depicted in the right column on the same scale and in the same format to allow for direct comparison with experiment.

In our work, we studied the properties of silver optical antennas fabricated in arrays displaced by approximately 5.4 nm from indium gallium arsenide (InGaAs) quantum well, grown by our group using molecular beam epitaxy, as pictured in figure 1 (a)(b) for an array of staggered wire-shaped antennas. We were concerned primarily with the effective coupling of the antenna array to the quantum well and used a simple toy-model [2] based on near-field coupling to explain the experimental observations. Using a transient frequency resolved pump-probe experiment, we measure the differential transmission of the system, revealing the expected signs of coupling. This experiment uses a femtosecond Ti:Sapphire laser at 810 nm to invert the quantum well, while an OPO tunable from 1360 nm to 1580 nm allows us to probe the changing transmission of the coupled system. We explore several areas of interest, including the effects of high pump power which causes the quantum well to act as a continuum of states rather than a single resonance. In this regime our simple toy model is no longer valid, and new features of the coupling are observed. Finally, we compare the optical properties and effective coupling of three distinct optical antenna shapes: wire, square and split-ring.

Figure 4 demonstrates the differential transmission response when the quantum well is pumped with only 4 mW, which should be just enough power to invert the lowest energy resonance of the

quantum well. The solid blue curves show the response of the quantum well by itself, and the dashed red curves show the response of the quantum well coupled to the wire antenna array. From this data we see a magnitude of the negative signal of about -3.8%. Also, for most wavelengths we see a nearly exponential decay, and the initial rise (fall) time is consistent, reaching a maximum or minimum signal at +20 ps delay.

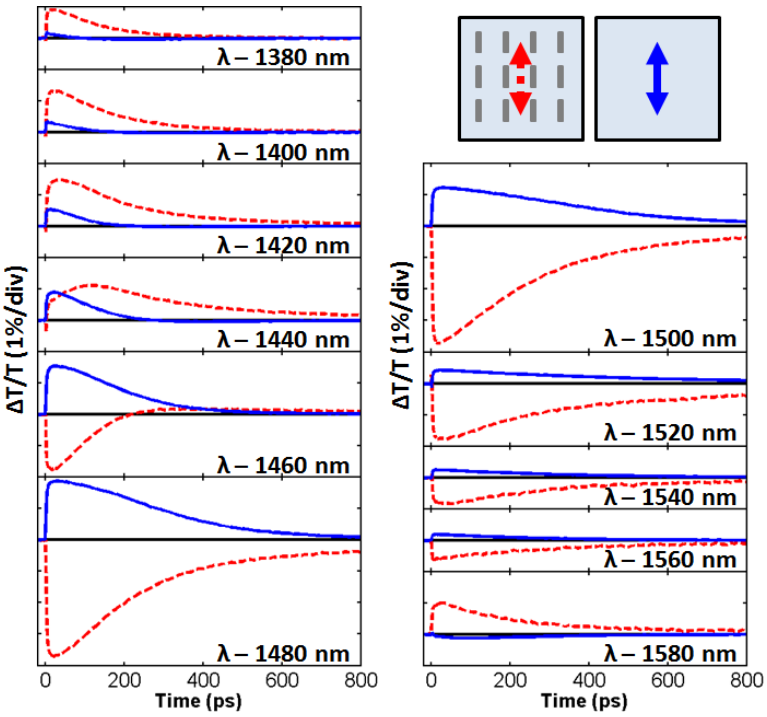

Figure 4: Transient pump-probe data collected from both the quantum well alone (solid blue) and from a resonant silver wire antenna array coupled to the quantum well (dashed red), for a pump power of 4 mW and probe wavelength ranging from 1380 nm to 1580 nm.

In order to compare this to previous work, we can use the toy model explained previously. To do this we first look at a single delay time corresponding to the maximum signal, when hot carriers have relaxed to the lowest energy level of the quantum well and the system can be approximated as steady state, which occurs around +20 ps. When we plot this time slice as a function of probe wavelength we get the plot seen in figure 5. Here again the blue data are the response of the quantum well and the red data are the response of the coupled system. The open circles are the experimental data, while the curves are the best fit to the toy model. All but one parameter in this model can be set from independent measurements of the quantum well and wire antenna array, leaving one free parameter, representing the strength of the coupling (L), which is varied to obtain this fit. The parameters for the quantum well and three different nano-antenna shapes are in table 1. From our fits, we observe good qualitative agreement with this model, confirming that for low excitation power the quantum well does indeed behave like a two-level system.

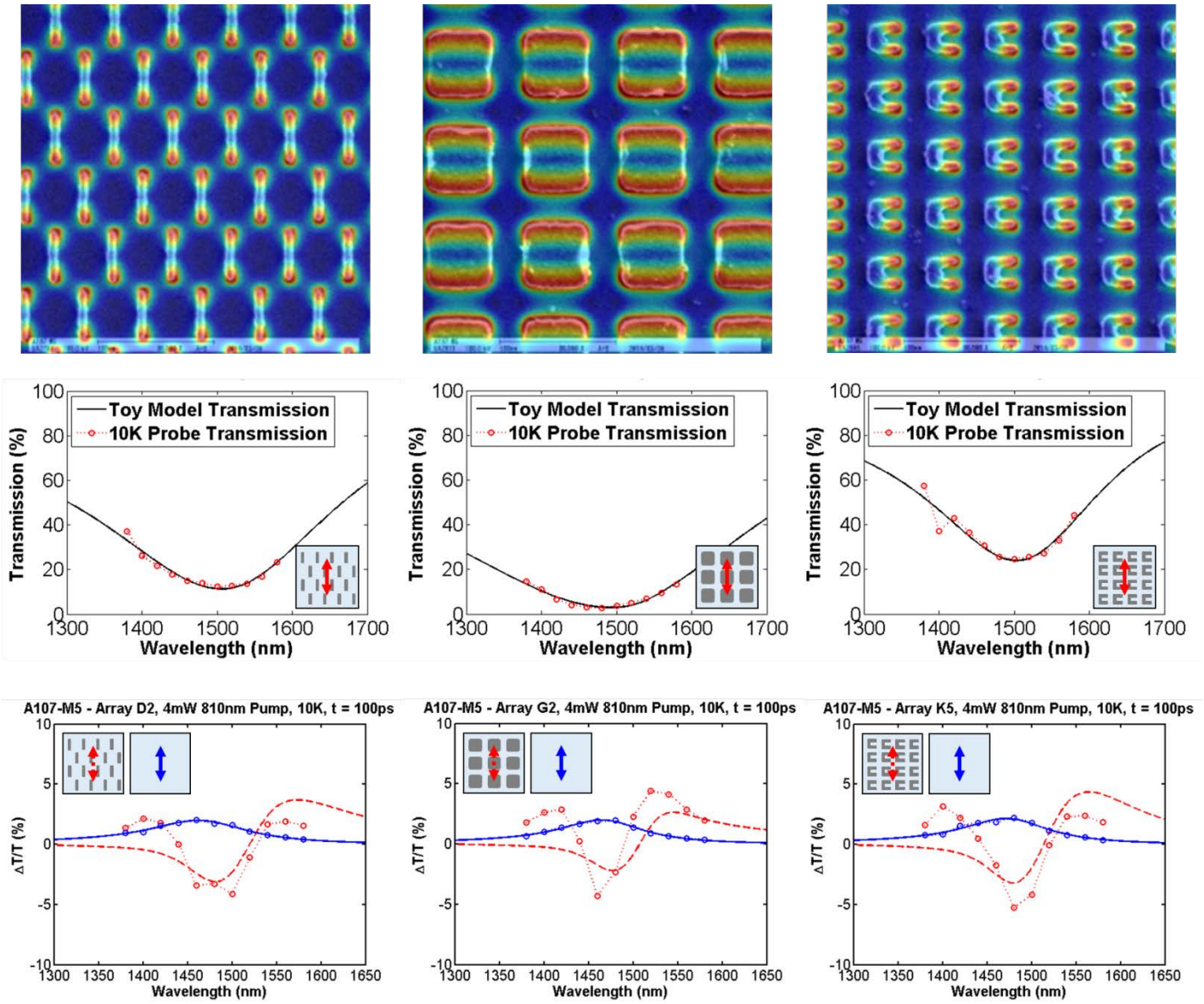

Figure 5: Row 1 shows the different nano-antenna shapes that were fabricated and studied, with electric field distribution overlaid. The E-field distribution was calculated with a FDTD simulation written by another group in our College. The transmission of each nano-antenna array in row 2 was measured and fit to extract important experimental parameters for use within the toy model .For each array differential transmission data were collected on the array and also from a region directly next to it with no antennas with an average pump power of 4 mW. These data are plotted in row 3. The data collected from the quantum well alone are shown in blue while the data from the coupled system are shown in red. Since all three arrays were fabricated during the same process on the same quantum well, the behavior of the quantum well (solid blue) was very similar for all three and the average parameters for the quantum well are summarized in the table below. With these parameters fixed, we vary the effective coupling parameter (*L*) in order to best match the differential transmission signal of the coupled system, shown by the dashed red curves above. *L* is summarized in the table below.

Table 1 – Summary of toy model parameters from fit to experimental data.

	Quantum Well	Wire Antennas	Square Antennas	Split-Ring Antennas
ω	2π x 204 THz	2π x 197 THz	2π x 198 THz	2π x 198 THz
γ	2π x 8.6 THz	2π x 9.4 THz	2π x 7.7 THz	2π x 9.7 THz
d	8.7 x 10^{-29} Cm	7.8 x 10^{-26} Cm	17 x 10^{-26} Cm	5.8 x 10^{-26} Cm
N	2.1 x 10^{24} m^{-3}	5.33 x 10^{20} m^{-3}	1.98 x 10^{20} m^{-3}	5.33 x 10^{20} m^{-3}
L		0.38 x 10^{10} mF^{-1}	0.18 x 10^{10} mF^{-1}	0.56 x 10^{10} mF^{-1}
V_{eff}		8.4 THz	5.0 THz	9.1 THz

Table 1: ω is the resonance frequency, γ is the damping frequency, d is the dipole moment, N is the density, L is the coupling parameter, and V_{eff} is the effective coupling frequency, which accounts for the dipole moment and density of the two systems.

From these fits, we found that the split-ring antennas show the greatest coupling, both in terms of the coupling parameter (L) and the effective coupling frequency (V_{eff}). Surprisingly, the square antennas which had the largest dipole moment show the smallest coupling. This can be explained by looking more closely at the toy model. Further discussion is contained within reference 1.

A Move Toward Quantum Dots

Naturally, following our in depth and systematic study of nano-antennas and quantum wells, we wanted to extend our investigation to the coupling of metallic resonators to quantum dots. From reference 9 and figure 2, we know that the field falls of exponentially from the surface, where the coupling is strongest at 5 nm or shallower, at 20 nm it's already at 20%, and at 40 nm from the surface, the coupling is essentially zero. Figure 6 shows a series of QD growths where the QD layer depth was varied. This series of QD growths demonstrated that we would be unable to grow high quality QDs close enough to the surface to couple to the near-field of our EBL fabricated metallic nano-antennas. We then attempted to passivate the near-surface samples with 1-2 nm layers of AlN and TiN. While this increased the emission of the ensemble of quantum dots, it still didn't result in high quality, distinct single QD emission lines. High quality quantum dots are grown in the 920 – 950 nm. Fabricating nano-antennas with resonances centered at a wavelength below 1 μm is non-trivial, even with state-of-the-art facilities.

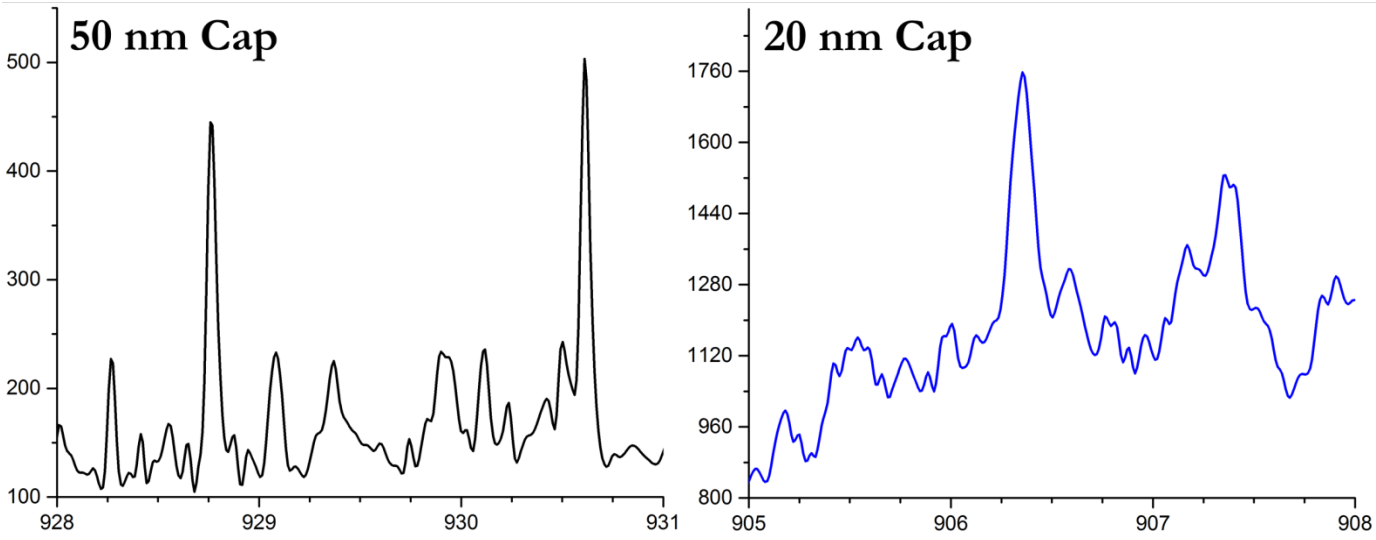

Figure 6: Here are two spectra demonstrating single quantum dot lines taken from samples where the quantum dot layers are at varying distances beneath the surface. The x-axis is wavelength in nanometers, and the y-axis arbitrary intensity units. It is thus clear that the deeper the quantum dots lie, the higher quality they are (*i.e.* narrower spectral lines). We also grew two samples where the quantum dots were 7.5 and 5.0 nm below the surface, but we were unable to resolve single quantum dot peaks.

Self-Assembled Indium Islands and Superconductivity

At around the same time, we successfully grew pure crystalline indium islands *in situ* on top of our semiconductor quantum-emitting heterostructures via MBE. This is a clean method of getting metallic structures near our quantum wells and dots without the need to remove our sample from the high vacuum chamber. This prevents the sample surface from being contaminated or oxidized while it is transported and prepared for lithography. The resulting indium islands are randomly-positioned, but the sizes, general shape, and density can be tuned by adjusting the MBE growth parameters.

Over 80 indium samples have been grown, and we have grown to understand their characteristics; *i.e.* which knobs to turn to alter the size, shape, and density. We showed that the photoluminescence can be enhanced if we grew QDs near a surface with indium islands, see figure 7 below.

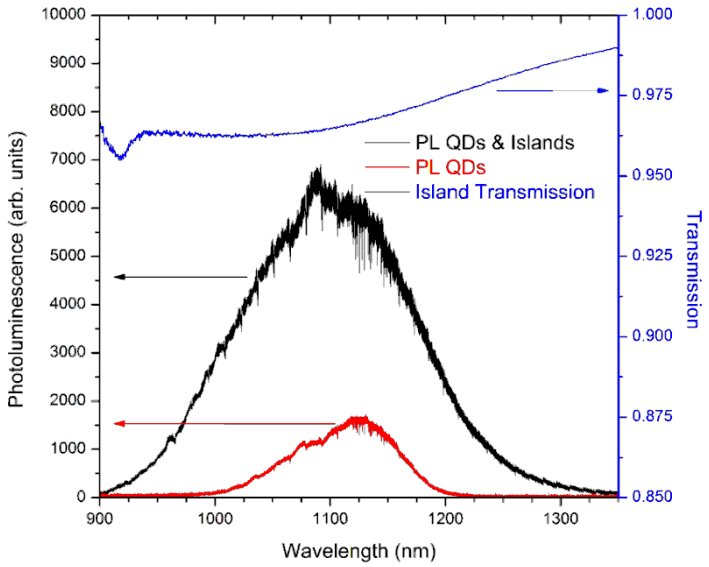

Figure 7: At 10.8 K, a 4x PL enhancement is measured between samples where indium islands, with an average density of ~1/μm^2, are grown on a GaAs/InAs QD sample with a 7 nm GaAs cap and a sample grown using the same parameters without indium islands.

An interesting property of bulk indium is its superconductivity just above 3 K. We wanted to verify that our mesoscale indium islands behaved in the same way, and we had the perfect tool to probe at such low temperatures, a Janis He^3 cryostat with a minimum temperature in the hundreds of millikelvin. This achievement is demonstrated in figure 8 [12]. The hope is that this discovery will allow us to utilize our epitaxially grown indium materials with superconducting properties on top of III-V semiconductor heterostructures, providing the cleanest possible interface for transferring coherence from superconducting electrons to semiconductor photon emission via the proximity effect. The proximity effect allows for electrons in the conduction band of a semiconductor in contact with a superconductor to occupy a superconducting like state. This would allow for entangled electron pairs (Cooper pairs) from the superconductor to radiatively recombine with holes in the semiconductor, producing entangled photons containing quantum state information from the original electrons [23].

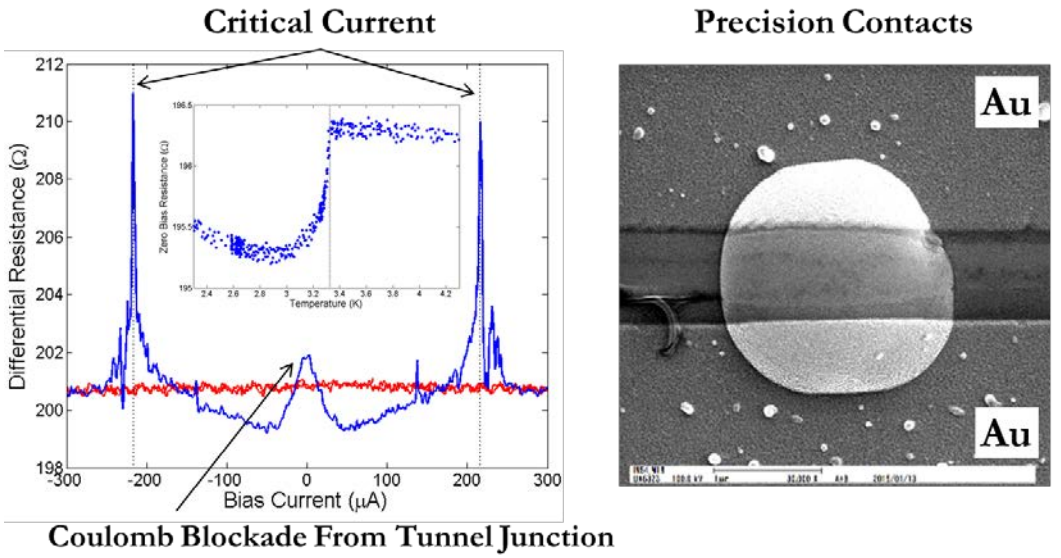

Figure 8: To verify superconductivity, we measured the resistance of a single indium island (*left*). Right Electron beam lithography is used to pattern gold contacts on the sample which precisely contact a single island (*right*). A drop in resistance was seen at a critical temperature of 3.325 K; a large resistance remains from the gold contacts (inset in left figure). Looking at differential resistance provides more detail, where peaks appear at the critical current. At higher currents, the island is no longer superconducting. The critical current is temperature dependent but is seen to be about 217 microamps at 0.44 K. A peak in resistance around zero bias current appears as the temperature is lowered. This is due to the native indium oxide layer that is between the indium island and gold contacts. This forms a tunnel barrier for electrons. As the temperature is decreased, electrons do not have enough thermal energy to tunnel through this barrier causing a rise in resistance.

Conclusion

The coupling of radiation emitted on semiconductor interband transitions to resonant optical-antenna arrays allows for enhanced light-matter interaction via the Purcell effect. Semiconductor optical gain also potentially allows for loss reduction in metamaterials. Over the past decade research based on optical antennas has grown quickly, with applications covering high resolution microscopy, single-photon sources, photo-voltaics, optical switching, metamaterials and more [13-20]. These studies have also led to many interesting theoretical questions on the nature of electro-magnetic fields confined by metallic nano-structures [21-23]. Our work with quantum wells and nano-antennas further elucidates the coupling behavior of these novel systems. While we weren't able to complete a similar investigation with quantum dots, we developed a growth procedure for self-assembled indium islands and investigated their optical, plasmonic, and superconducting properties. These exciting materials provide the platform for transfer of coherence between superconductors and semiconductors.

Personnel

Graduate students supported by this grant: Michael Gehl (Graduated with PhD in October 2015, now at Sandia National Laboratories), Ricky Gibson, Sander Zandbergen, Jasmine Sears, and Patrick Keiffer.

Professor: Galina Khitrova

References

1. M. Gehl, S. Zandbergen, R. Gibson, M. Béchu, N. Nader, J. Hendrickson, J. Sears, P. Keiffer, M. Wegener, and G. Khitrova, "Spectroscopic studies of resonant coupling of silver optical antenna arrays to a near-surface quantum well." J. Opt. **16**, 114016 (2014).
2. M. Wegener, J. L. Garcia Pomar, C. M. Soukoulis, N. Meinzer, M. Ruther, and S. Linden, "Toy model for plasmonic metamaterial resonances coupled to two-level system gain." Opt. Express **16**, 19785-19798 (2008).
3. S. Linden, C. Enkrich, M. Wegener, J. Zhou, T. Koschny, and C. M. Soukoulis, "Magnetic response of metamaterials at 100 Terahertz." Science **306**, 1351 (2004).
4. C. M. Soukoulis, S. Linden, and M. Wegener, "Negative refractive index at optical wavelengths," Science **315**, 47 (2007).
5. D. J. Bergman and M. I. Stockman, "Surface plasmon amplification by stimulated emission of radiation: quantum generation of coherent surface plasmons in nanosystems," Phys. Rev. Lett. **90**, 027402 (2003).
6. T. Yoshie, A. Scherer, J. Hendrickson, G. Khitrova, H. M. Gibbs, G. Rupper, C. Ell, O. B. Shchekin, and D. G. Deppe, "Vacuum Rabi splitting with a single quantum dot in a photonic crystal nanocavity." Nature **432**, 200-203 (2004).
7. G. Khitrova, H. M. Gibbs, M. Kira, S. W. Koch, and A. Scherer, "Vacuum Rabi splitting in semiconductors." Nature Physics **2**, 81 (2006).
8. G. Khitrova, H. M. Gibbs, F. Jahnke, M. Kira, and S. W. Koch, "Nonlinear optics of normal-mode coupling semiconductor microcavities." Rev. Mod. Phys. **71**, 1591 (1999).
9. N. Meinzer, M. König, M. Ruther, S. Linden, G. Khitrova, H. M. Gibbs, K. Busch, and M. Wegener, "Distance-dependence of the coupling between split-ring resonators and single-quantum-well gain." Appl. Phys. Lett. **99**, 111104 (2011).
10. N. Meinzer, M. Ruther, S. Linden, C. M. Soukoulis, G. Khitrova, J. Hendrickson, J. D. Olitzky, H. M. Gibbs, and M. Wegener, "Arrays of Ag split-ring resonators coupled to InGaAs single-quantum-well gain." Opt. Express **18** (23), 24140-24151 (2010).
11. M. Husnik, S. Linden, R. Diehl, J. Niegemann, K. Busch, and M. Wegener, "Quantitative Experimental Determination of Scattering and Absorption Cross-Section Spectra of Individual Optical Metallic Nanoantennas." Phys. Rev. Lett. **109**, 233902 (2012).

12. M. Gehl, R. Gibson, S. Zandbergen, P. Keiffer, J. Sears, and G. Khitrova, "Superconductivity in epitaxially grown self-assembled indium islands - Progress towards hybrid superconductor/semiconductor optical sources." Submitted to JOSA B, Feb 2016.
13. P. Biagioni, J.-S. Huang, and B. Hecht, "Nanoantennas for visible and infrared radiation." Rep. Prog. Phys. **75**, 024402 (2012).
14. J. N. Farahani, H. J. Eisler, D. W. Pohl, M. Pavius, P. Flückiger, P. Gasser, and B. Hecht, "Bow-tie optical antenna probes for single-emitter scanning near-field optical microscopy." Nanotechnology **18**, 125506 (2007).
15. A. V. Akimov, A. Mukherjee, C. L. Yu, D. E. Change, A. S Zibrov, P. R. Hemmer, H. Park, and M. D. Lukin, "Generation of single optical plasmons in metallic nanowires coupled to quantum dots." Nature **450**, 402 (2007).
16. A. G. Curto, G. Volpe, T. H. Taminiau, M. P. Kreuzer, R. Quidant, and N. F. van Hulst, "Unidirectional emission of a quantum dot coupled to a nanoantenna." Science **329**, 930 (2010).
17. L. Cao, P. Fan, A. P. Vasudev, J. S. White, Z. Yu, W. Cai, J. A. Schuller, S. Fan, and M. L. Brongersma, "Semiconductor nanowire optical antenna solar absorbers." Nano Lett. **10**, 439 (2010).
18. X. Fang, M. L. Tsend, J.-U. Ou, K. F. MacDonald, D. P. Tsai, and N. I. Zheludev, "Ultrafast all-optical switching via coherent modulation of metamaterial absorption." Appl. Phys. Lett. **104**, 141102 (2014).
19. O. Hess, J. B. Pendry, S. A. Maier, R. F. Oulton, J. M. Hamm, and K. L. Tsakmakidis, "Active nanoplasmonic metamaterials." Nature Mat. **11**, 574-584 (2012).
20. N. Kumar, "Spontaneous Emission Rate Enhancement Using Optical Antennas." Ph.D. Dissertation, Electrical Engineering and Computer Sciences, UC Berkeley, Berkeley, CA (2013).
21. J.-J. Greffet, M. Laroche, and F. Marquier, "Impedance of a Nanoantenna and a Single Quantum Emitter." Phys. Rev. Lett. **105**, 117701 (2010).
22. S. A. Maier, "Plasmonic field enhancement and SERS in the effective mode volume picture." Opt. Express **14**, 1957 (2006).
23. A. F. Koenderink, "On the use of Purcell factors for Plasmon antennas." Opt. Lett. **35**, 4208 (2010).

Publications

1. P. R. Berman, S. R. Zandbergen, and G. Khitrova, "Vertical dipole above a dielectric or metallic half-space - energy flow considerations." Phys. Rev. E **92**, 013203 (2015).
2. R. Gibson, M. Gehl, J. Sears, S. Zandbergen, N. Nader, P. Keiffer, J. Hendrickson, A. Arnoult, and G. Khitrova, "Molecular beam epitaxy grown indium self-assembled plasmonic nanostructures." J. Cryst. Growth, **425**, 307-311 (2015).
3. B. L. Wilmer, F. Passmann, M. Gehl, G. Khitrova, and A. D. Bristow, "Multidimensional coherent spectroscopy of a semiconductor microcavity." Phys. Rev. B **91**, 201304 (2015).

4. M. Gehl, S. Zandbergen, R. Gibson, M. Béchu, N. Nader, J. Hendrickson, J. Sears, P. Keiffer, M. Wegener, and G. Khitrova, "Spectroscopic studies of resonant coupling of silver optical antenna arrays to a near-surface quantum well." J. Opt. **16**, 114016 (2014).
5. M. Teich, M. Wagner, D. Stehr, H. Schneider, M. Helm, C. N. Böttge, A. C. Klettke, S. Chatterjee, M. Kira, S. W. Koch, G. Khitrova, and H. M. Gibbs. "Systematic investigation of terahertz-induced excitonic Rabi splitting." Phys. Rev. B, **89**, 115311 (2014).
6. A. C. Klettke, M. Kira, S. W. Koch, J. L. Tomaino, A. D. Jameson, Y.-S. Lee, G. Khitrova, and H. M. Gibbs, "Terahertz excitations of lambda systems in a semiconductor microcavity." Phys. Status Solidi C, **10**, 1222-1225 (2013).
7. B. Ewers, N. S. Köster, R. Woscholski, M. Koch, S. Chatterjee, G. Khitrova, H. M. Gibbs, A. C. Klettke, M. Kira, and S. W. Koch, "THz-manipulation of excitonic polarization in (GaIn)As/GaAs quantum wells." Phys. Status Solidi C, **10**, 1226-1229 (2013).
8. W. D. Rice, J. Kono, S. Zybell, S. Winner, J. Bhattacharyya, H. Schneider, M. Helm, B. Ewers, A. Chernikov, M. Koch, S. Chatterjee, G. Khitrova, H. M. Gibbs, L. Schneebeli, B. Breddermann, M. Kira, and S. W. Koch, "Observation of Forbidden Exciton Transitions Mediated by Coulomb Interactions in Photoexcited Semiconductor Quantum Wells." Phys. Rev. Lett., **110**, 137404 (2013).
9. I. Avrutsky, R. Gibson, J. Sears, G. Khitrova, H.M. Gibbs, and J. Hendrickson, "Linear systems approach to describing and classifying Fano resonances." Phys. Rev. B, **87**, 125118 (2013).

Conference Proceedings

1. R. Gibson, M. Gehl, S. Zandbergen, P. Keiffer, J. Sears, G. Khitrova, "Progress of the quantum nano-optics of semiconductors group at Optical Sciences." Proc. SPIE 9186, Fifty Years of Optical Sciences at The University of Arizona, 91860F (September 5, 2014).

Presentations

1. M. Gehl, R. Gibson, S. Zandbergen, J. Sears, N. Nader, P. Keiffer, J. Hendrickson, A. Arnoult, G. Khitrova, "Observation of Superconductivity in Self-Assembled Indium Island Epitaxially Grown on top of III-V Semiconductors," APS/DLS Laser Science, San Jose, CA, October 2015.
2. G. Khitrova, "Indium/InAs Majorana Qubits Capable of Emitting Photons." Beyond Exascale: Qubits for Quantum Computing Workshop, Oak Ridge National Labs, TN, August 2015.
3. G. Khitrova, "Shipwrecked on an Indium Island in Search of Majorana Fermions." Fundamental Optical Processes in Semiconductors 2015, Breckenridge, CO, August 2015.
4. M. Gehl, S. Zandbergen, R. Gibson, M. Béchu, N. Nader, J. Hendrickson, J. Sears, P. Keiffer, M. Wegener, G. Khitrova, "Effect of Metallic Antenna Shape on the Near-Field Coupling to a Semiconductor Quantum Well," APS/DLS Laser Science, Tucson, AZ, October 2014.

5. R. Gibson, S. Zandbergen, M. Gehl, J. Sears, N. Nader, P. Keiffer, J. Hendrickson, M. Wegener, G. Khitrova, "In Situ Growth of Self-Assembled Indium Islands in Close Proximity to Semiconductor Quantum Emitters." APS/DLS Laser Science, Tucson, AZ, October 2014.
6. S. Zandbergen, R. Gibson, M. Gehl, J. Sears, N. Nader, P. Keiffer, E. Müller, H. Störmer, D. Gerthsen, J. Hendrickson, M. Wegener, A. Arnoult, G. Khitrova, "Resonant Coupling of Self-Assembled Crystalline Indium Islands to III-V Heterostructure." Nonlinear Optics and Excitation Kinetics in Semiconductors, Bremen, Germany, September 2014.
7. R. Gibson, M. Gehl, S. Zandbergen, J. Sears, N. Nader, P. Keiffer, E. Müller, H. Störmer, D. Gerthsen, J. Hendrickson, A. Arnoult, G. Khitrova, "MBE Grown Indium Self-Assembled Plasmonic Structures." 18th International Conference on Molecular Beam Epitaxy, Flagstaff, AZ, September 2014.
8. G. Khitrova, M. Gehl, S. Zandbergen, M. Béchu, R. Gibson, J. Sears, M. Wegener, "Nonlinear Behavior of Metallic Antennae Resonantly Coupled to a Quantum Well." Fundamental Optical Processes in Semiconductors, Kodiak Island, AK, August 2013.
9. M. Gehl, S. Zandbergen, M. Béchu, R. Gibson, J. Sears, M. Wegener, G. Khitrova, "Nonlinear Behavior of Metallic Antennae Resonantly Coupled to a Quantum Well." Nonlinear Optics, Kohala Coast, HI, July 2013.

Interactions/Transitions

Publications, talks at various meetings, posters (not included), and discussions with multiple visitors constitute the technology transfer for this project.

Patents

None.